american physiological society

JNP JOURNAL OF NEUROPHYSIOLOGY

J Neurophysiol 125: 1095–1110, 2021.
First published February 3, 2021; doi:10.1152/jn.00350.2019

RESEARCH ARTICLE

Sensory Processing

Integration of vestibular and hindlimb inputs by vestibular nucleus neurons: multisensory influences on postural control

Andrew A. McCall,[1]* Derek M. Miller,[1]* and Carey D. Balaban[1,2,3,4]

[1]*Department of Otolaryngology, University of Pittsburgh, Pittsburgh, Pennsylvania;* [2]*Department of Neurobiology, University of Pittsburgh, Pittsburgh, Pennsylvania;* [3]*Department of Communication Sciences and Disorders, University of Pittsburgh, Pittsburgh, Pennsylvania; and* [4]*Department of Bioengineering, University of Pittsburgh, Pittsburgh, Pennsylvania*

Abstract

We recently demonstrated in decerebrate and conscious cat preparations that hindlimb somatosensory inputs converge with vestibular afferent input onto neurons in multiple central nervous system (CNS) locations that participate in balance control. Although it is known that head position and limb state modulate postural reflexes, presumably through vestibulospinal and reticulospinal pathways, the combined influence of the two inputs on the activity of neurons in these brainstem regions is unknown. In the present study, we evaluated the responses of vestibular nucleus (VN) neurons to vestibular and hindlimb stimuli delivered separately and together in conscious cats. We hypothesized that VN neuronal firing during activation of vestibular and limb proprioceptive inputs would be well fit by an additive model. Extracellular single-unit recordings were obtained from VN neurons. Sinusoidal whole body rotation in the roll plane was used as the search stimulus. Units responding to the search stimulus were tested for their responses to 10° ramp-and-hold roll body rotation, 60° extension hindlimb movement, and both movements delivered simultaneously. Composite response histograms were fit by a model of low- and high-pass filtered limb and body position signals using least squares nonlinear regression. We found that VN neuronal activity during combined vestibular and hindlimb proprioceptive stimulation in the conscious cat is well fit by a simple additive model for signals with similar temporal dynamics. The mean R^2 value for goodness of fit across all units was 0.74 ± 0.17. It is likely that VN neurons that exhibit these integrative properties participate in adjusting vestibulospinal outflow in response to limb state.

NEW & NOTEWORTHY Vestibular nucleus neurons receive convergent information from hindlimb somatosensory inputs and vestibular inputs. In this study, extracellular single-unit recordings of vestibular nucleus neurons during conditions of passively applied limb movement, passive whole body rotations, and combined stimulation were well fit by an additive model. The integration of hindlimb somatosensory inputs with vestibular inputs at the first stage of vestibular processing suggests that vestibular nucleus neurons account for limb position in determining vestibulospinal responses to postural perturbations.

limb; sensory integration; vestibular

INTRODUCTION

The maintenance of balance is an inherently multimodal process. The central nervous system (CNS) integrates information from vestibular (1–4), visual (5–8), and proprioceptive (3, 9–12) sensors to generate an estimate of body position and movement in space and to shape corrective postural responses to perturbations (13, 14). The integration of multimodal input streams underlying the neural control of posture remains an active area of research. Early data from human studies suggested that sensory inputs (in large part) sum linearly to generate effector responses (14–16). More recent data suggest that nonlinearities exist, such that the CNS "reweights" these sensory inputs depending upon input stimulus conditions (14, 17). Attention to perceptual inputs from both goal-driven attentional demands and exogenous stimulus-driven factors also influences multisensory processing, including maintenance of posture (18–20).

*A. A. McCall and D. M. Miller contributed equally to this work.
Correspondence: A. A. McCall (mccallaa@upmc.edu).
Submitted 6 June 2019 / Revised 15 December 2020 / Accepted 28 January 2021

In addition to being probed at the level of the whole organism through measuring output responses to perturbations (e.g., postural sway data), multimodal integration has been documented among populations of neurons (e.g., in fMRI and EEG studies) and at the single neuron level (21). At the single unit neuron level, multisensory integration sometimes results in an output that represents a straightforward, linear summation of responses to different sensory modalities and submodalities (22). In other circumstances, multisensory integration (and in some situations of repeated sensory stimulation or during voluntary movement) responses can be dramatically attenuated or "gated" (22–25). In yet other circumstances, super-additivity may occur, whereby responses are enhanced well beyond those seen when one input is activated alone (26–28).

Although there are multiple sites in the brainstem that process inputs from the vestibular, visual, and somatosensory systems, the vestibular nuclei (VN) are of particular importance because they function as key sensory integrators that govern many reflexes relevant to the maintenance of balance, such as vestibulo-ocular and vestibulospinal reflexes (29). Although it has long been appreciated that VN neurons are the site of first synapse of most peripheral vestibular afferents and receive strong proprioceptive projections from the neck, recent work has demonstrated that proprioceptive inputs from the limbs influence VN neuronal firing as well (30, 31).

Previous work in the decerebrate cat model has shown that many vestibular nucleus neurons respond to convergent vestibular afferent and neck proprioceptive afferent inputs in an additive fashion. Response properties of the individual components (opposing vector orientations, similar sensitivity, and phase dynamics) are well-suited to sum linearly and therefore cancel out when coactivated, which has been shown in decerebrate cats during head-on-body movements which simultaneously activate both receptors (32). Similar findings have been confirmed in some species of conscious nonhuman primates (33), but not others (34).

Our objective was to determine how VN neurons integrate convergent vestibular and limb proprioceptive inputs. The processing of inputs from these sources is perhaps more complex than those from vestibular and neck proprioceptive inputs. Coactivation of vestibular and neck proprioceptive inputs would be expected to be tightly coupled because, by necessity, nearly all head movements during ordinary activity will result in coactivation of vestibular and neck proprioceptive inputs. A similar tight coupling of vestibular and limb proprioceptive inputs would be expected in some circumstances, such as during ambulation, because head movements are patterned with the step cycle (35). In contrast, other movements of the weight-bearing limbs would not be expected to have a predictable or appreciable effect on head movement, such as standing in place and raising one leg. Therefore, the processing of proprioceptive information from different areas of the body may be handled differently in the vestibular nuclei. We hypothesized that VN neuronal firing during activation of vestibular and limb proprioceptive inputs in conscious cats would be well fit by an additive model. Cats were selected for this study because they have served well as models for vestibular neurophysiology experiments [e.g., Miller et al. (36) and Wilson et al. (37)], limb proprioceptive and locomotion experiments [e.g., Abelew et al. (38) and Frigon and Rossignol (39)], and are the animal model in which vestibular and limb proprioceptive inputs have been shown to converge in brainstem centers, including the VN (30, 31, 40, 41). Conscious cats were selected over decerebrates because considerable differences in modulation of neuronal firing in the brainstem have been seen with decerebration, including in the VN in response to limb movement (31, 42).

Here, we report results of in vivo recordings from single VN neurons in conscious cats in response to whole body trapezoid rotation in the roll plane (vestibular stimulation), hindlimb movement in the sagittal plane (limb proprioceptive stimulation), and during simultaneous delivery of both vestibular and limb stimuli. For each neuron, composite response histograms were generated and fit by a model of low- and high-pass filtered limb and vestibular signals using least squares nonlinear regression. We found that VN neuronal firing was explained by an additive model that incorporated subcomponents of the stimuli. We speculate that VN neurons that exhibit these integrative properties participate in adjusting vestibulospinal outflow in response to limb state.

METHODS

Experimental protocols were reviewed and approved by the University of Pittsburgh's Institutional Animal Care and Use Committee and conformed to the National Research Council Guide for the Care and Use of Laboratory Animals (National Academies Press, Washington, DC, 2011). Data were collected from four purpose-bred spayed female cats obtained from Liberty Research (Waverly, NY) that were instrumented for chronic extracellular single-unit recordings using procedures described in previous publications (36, 40, 41, 43). These procedures will be summarized succinctly under *Surgical Procedures* below.

Surgical Procedures

After a period of acclimation for restraint, each animal underwent a recovery surgery conducted under aseptic conditions in a dedicated operating suite. Animals were initially anesthetized using an intramuscular injection of ketamine (20 mg/kg) and acepromazine (0.2 mg/kg). Animals were intubated, and anesthesia was maintained using isoflurane (1%–2%) vaporized in oxygen. An intravenous catheter was inserted in the forelimb and saline was infused intravenously to address fluid loss. A heating pad and an infrared heat lamp were used to maintain the core temperature between 36°C and 38°C. A midline 1 cm craniotomy was made in the posterior aspect of the skull centered over the vestibular nuclei using stereotactic coordinates. A recording chamber (David Kopf Instruments, Tujunga, CA) was centered over the craniotomy and anchored to the skull using stainless steel screws and Palacos bone cement (Zimmer, Warsaw, IN). Rostral to the recording chamber, a fixation plate was mounted to the skull in a similar fashion. Electromyographic (EMG) patch electrodes were sutured to the biceps femoris and vastus lateralis muscles of both limbs through incisions on the lateral aspect of the thigh; leads were routed subcutaneously to a connector mounted on the skull. One of the four animals had significant bleeding from the cerebellum at the time of craniotomy requiring repeated application of hemostatic agents;

after the surgery, the animal was posturally unsteady for several weeks. Postmortem histological examination demonstrated partial degeneration of the cerebellar cortex ipsilateral to the recording site. Despite this injury, the single unit data from the VN of this animal were indistinguishable from those obtained from the other three animals and thus were included in this report. Furthermore, the animal's posture and gait improved to the point where there was no evident behavioral difference with the other animals, and recordings were not commenced until after this recovery had occurred. Postsurgical analgesia was provided continuously for 72 h through a transdermal fentanyl delivery system (25 μg/h, Janssen Pharmaceutical Products, Titusville, NJ). Amoxicillin (50 mg, twice a day) was administered orally for 10 days following surgery.

Vestibular Stimulation and Hindlimb Movement Protocols

Animals were acclimated over a period of several weeks to head and body restraint while table movements and hindlimb ramp-and-hold movements were applied. The animal was placed in a modified restraint bag (Four Flags Over Aspen, Aspen, CO) with a hole cut in the rear to allow access to the hindlimb. The hindlimb was secured via a Velcro strap placed at the ankle to a servocontrolled motor capable of delivering movements in the rostral-caudal axis (i.e., hindlimb extension and flexion). The torso was fit snugly into a padded cylindrical tube secured to the stereotaxic frame, and straps were placed around the animal's body to snugly secure the animal. The head was immobilized by attaching the fixation plate to a post mounted on the stereotaxic frame. The stereotaxic frame was mounted atop a servocontrolled hydraulic tilt table (NeuroKinetics, Pittsburgh, PA) capable of delivering movements in the pitch and roll planes (Fig. 1).

Sinusoidal whole body rotation in the roll plane was used as the search stimulus to identify neurons receiving vestibular afferent input (Fig. 2). Units responding to the search stimulus were evaluated further for responses during three conditions in succession (hereafter referred to as integration trials): *1*) ramp-and-hold body roll rotation; *2*) ramp-and-hold leg extension; and *3*) simultaneously delivered ramp-and-hold body roll and leg extension (Fig. 3). Maximum displacement during the hold segment of body roll and leg extension was 10° and 60°, respectively. Each trial incorporating all three conditions was 18 s in duration with each ramp phase lasting 1 s and each hold phase lasting 2 s. These stimulation parameters were chosen because prior experiments demonstrated that they produce robust modulation of VN neurons in the conscious cat (31, 36). In most instances, ten trials were repeated for each isolated neuron. In some instances, a given unit was lost before completion of all trials; neurons with fewer than five trials were excluded from analysis. During most trials, animals permitted passive hindlimb movement, as there was no change in hindlimb muscle EMG activity, and the limb movement recorded from a potentiometer on the servomotor was identical to the command signal provided by the computer controlling the servomotor. Trials in which EMG activity increased over baseline during the hindlimb movement or where the hindlimb movement deviated from that delivered by the servomotor were excluded from the analyses described below (see *Iterative Strategy for Vestibular and Limb Signal Identification*).

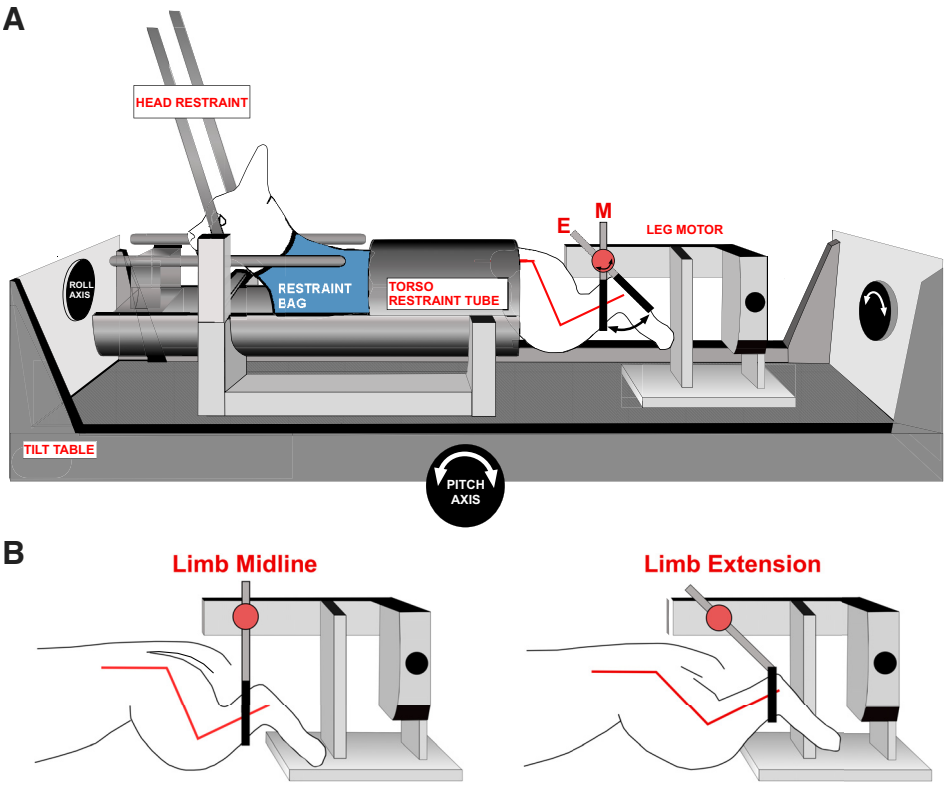

Figure 1. *A*: awake felines were placed into a restraint device mounted on a servocontrolled tilt table. The two-axis tilt table was used to provide vestibular stimulation by rotating the animal in the roll plane. *B*: a servocontrolled motor positioned behind the animal provided hindlimb movement. The hindlimb was placed through a hole in the restraint bag and secured to the servocontrolled motor via a Velcro strap attached immediately proximal to the ankle. Hindlimb position at midline and extension, with relative angles of the knee and hip joints, are shown. [Figure modified and reproduced from Ref. 41 with permission from Springer.]

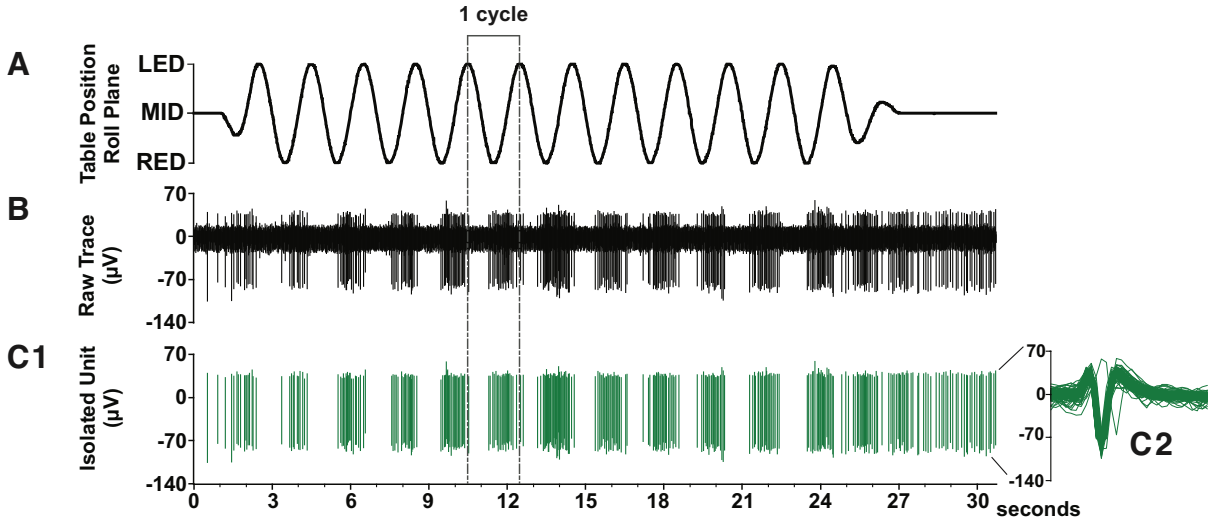

Figure 2. Example of a single vestibular nucleus (VN) neuron whose activity was robustly modulated by the search stimulus. *A*: sinusoidal whole body rotation in the roll plane was used as the search stimulus to identify neurons that received vestibular inputs (tilt frequency, 0.5 Hz; tilt amplitude, 5°). *B*: raw neural data sampled at 25 kHz. *C1*: tracing showing the isolated neuron of interest. *C2*: the overlaid spike-sorted waveforms were equivalent across all the trial, indicating that activity was sampled from the same neuron throughout the recording.

Neural Recording Procedures

Extracellular recordings were made from VN neurons using 4–6 MΩ epoxy-insulated tungsten microelectrodes (Frederick Haer, Bowdoin, ME). An XY positioner (David Kopf Model 608B) was secured atop the recording chamber, and the electrode was introduced via a 25-gauge stainless steel guide tube inserted through the dura and into the cerebellum. The electrode was lowered into the medulla using a hydraulic microdrive (David Kopf Model 650). Neural activity was amplified by a factor of 1 K or 10 K, bandpass filtered 0.3–10 kHz and sampled at 25 kHz using a Cambridge Electronic Design Micro 1401 mk2 data collection system and Spike 2 v. 8 software (Cambridge, UK). EMG data from the hindlimb musculature were amplified by 1,000, bandpass filtered 0.01–10 kHz and sampled at 1 kHz. Signals from potentiometers on the tilt table and servocontrolled leg motor provided body and hindlimb position, respectively, and were each sampled at 100 Hz.

Iterative Modeling Strategy for Vestibular and Limb Signal Identification

Spike occurrences were binned at 10-ms intervals and converted into instantaneous spike rates by dividing by the number of stimulus cycles and multiplying by 100. The table and limb position traces were centered at zero. The table and

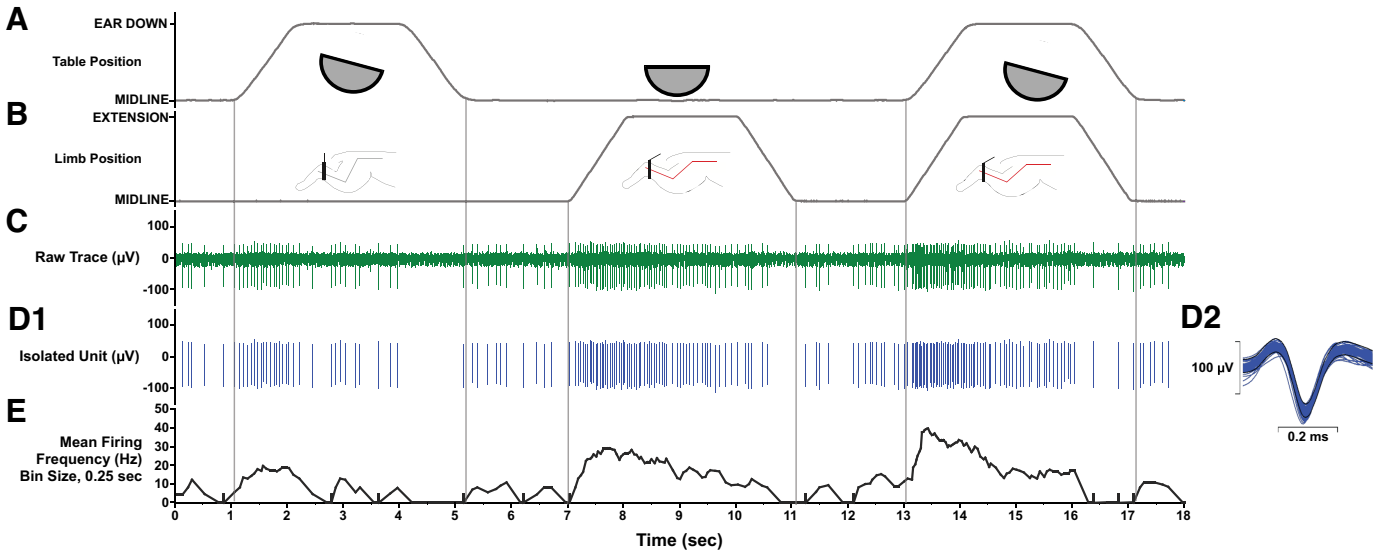

Figure 3. Units responding to the vestibular search stimulus were further tested for their responsiveness to 10° ramp-and-hold roll body and head rotation (*A*), 60° ramp-and-hold hindlimb extension movement (*B*), and both movements delivered simultaneously. *C*: raw neural data were sampled at 25 kHz. *D1:* unit activity was isolated using template-matching and response histograms were generated and fit by a model of low and high pass filtered limb and body position and velocity signals using least squares nonlinear regression. *D2*: the average spike-sorted waveforms (insets on right) were equivalent across the trial, indicating that activity was sampled from the same neuron throughout the recordings. *E*: mean firing frequency (bin width, 0.25 s).

limb velocities were calculated with the "gradient.m" function in MATLAB (The MathWorks, Natick, MA) at the 100 Hz sample rate. The limb position, limb velocity, table roll position, table roll velocity, and unit response data were then decimated to a 20 Hz rate using the MATLAB "decimate.m" function for model estimation. The first step in analysis was generation of a formal, parametric description of dynamic signal processing by these units. The MATLAB function "lsim.m" was used to implement low pass (LP) and high pass (HP) representations of the limb and table stimulus position and velocity traces, with simple first order transfer functions of $\frac{1}{0.5s+1}$ and $\frac{0.5s}{0.5s+1}$, respectively. The spike rate data sets were then fitted as a weighted linear sum of a baseline firing rate and direction sensitivities for the low pass (LP) and high pass (HP) roll position, HP roll velocity, LP and HP limb position, and LP and HP limb velocity, with sensitivities estimated by the MATLAB "lsqnonlin.m" function (Levenberg–Marquardt nonlinear least squares optimization). These models assumed additivity of all signals for the entire stimulus presentation period (roll alone, limb alone, then roll plus limb). Further statistical analysis was conducted in either SPSS v. 25 (with R and Python extensions) or in MATLAB.

An iterative strategy was followed to identify an uncorrelated set of vestibular and proprioceptive signals as linear combinations of the initial set of 13 signal components. The initial optimization step produced parameter estimates for the following:

1) baseline activity (a constant),
2) HP limb position sensitivity for extension,
3) HP limb position sensitivity for return to midline (hereafter "flexion"),
4) HP limb velocity sensitivity for extension,
5) HP limb velocity sensitivity for flexion,
6) LP roll position sensitivity for ipsilateral ear up rotation,
7) LP roll position sensitivity for ipsilateral ear down rotation,
8) HP roll position sensitivity for ipsilateral ear up rotation,
9) HP roll position sensitivity for ipsilateral ear down rotation,
10) LP limb position sensitivity for extension,
11) LP limb position sensitivity for flexion,
12) HP roll velocity sensitivity for ipsilateral ear up rotation, and
13) HP roll velocity sensitivity for ipsilateral ear down rotation.

Exploratory examination of the scatterplot matrix (Fig. 4) of these parameters for all units, validated by linear regression analysis, showed the following strong linear dependencies between components:

1) The high pass roll position sensitivities in the ipsilateral ear down and ipsilateral ear up sensitivities were highly correlated (adjusted $R^2 = 0.959$). The linear relationship was:

HP roll position down sensitivity = $-0.955 \times$ HP roll position up sensitivity $+ 0.104$.

Given the high R^2, the negligible intercept parameter, and a slope that does not differ from -1, high pass roll position was represented as a fully rectified process (i.e., responses to ear up and ear down roll have the same polarity and

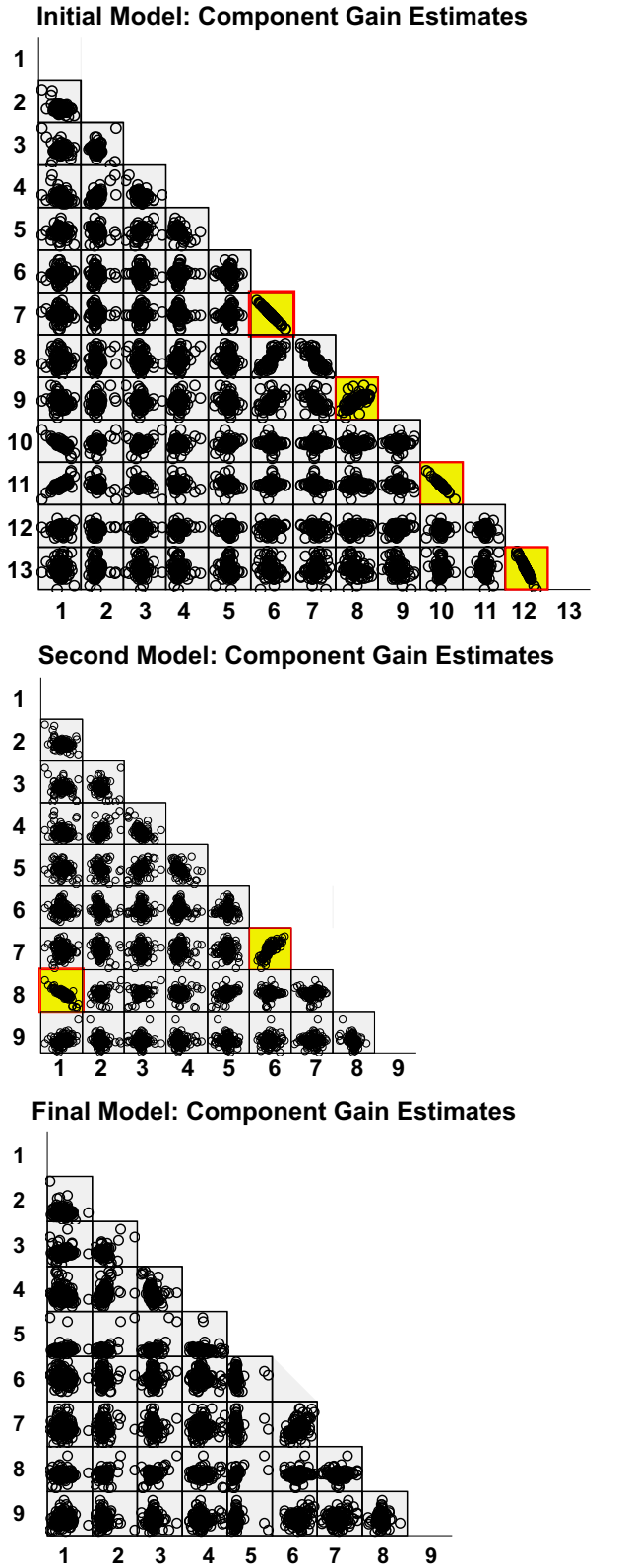

Figure 4. Iterative scatterplot matrices of model component estimates. The initial (*top*), second (*middle*), and final (*bottom*) scatterplot matrices are shown. Linear correlations (validated by regression modeling) are highlighted in yellow. Numbered parameters for each model iteration correspond to those shown in the METHODS.

magnitude) with a single sensitivity parameter for the second iteration.

2) The LP roll position sensitivities in the ipsilateral ear down and ipsilateral ear up sensitivities were highly correlated (adjusted R^2 = 0.910). The linear relationship was given by:

LP roll position down sensitivity = −0.896 × LP roll position up sensitivity + 0.027.

Because the R^2 is very high, the slope that does not differ from −1 and the estimated intercept is negligible, low pass roll position was represented as a fully rectified process with a single sensitivity parameter for the second iteration.

3) The LP limb position for flexion and extension sensitivities were highly correlated (adjusted R^2 = 0.908). The linear relationship was described by:

LP limb flexion position sensitivity = −1.017 × LP limb extension position sensitivity − 0.222.

As in the case of low pass roll position, the R^2 is very high, the slope that does not differ from −1, and the estimated intercept is negligible. Hence, low pass limb position was represented as a fully rectified process with a single sensitivity parameter for the second iteration.

4) The high pass roll velocity sensitivities in the ipsilateral ear down and ipsilateral ear up sensitivities were correlated significantly, but to a lesser degree (adjusted R^2 = 0.437). The linear relationship was:

HP roll velocity down sensitivity = 0.531× HP roll velocity up sensitivity − 0.099.

As a result, a single unrectified high pass roll velocity sensitivity process was implemented in the next iteration of the model.

The "second iteration" began with a new least squares estimation of parameters for representing the unit responses as a weighted sum of nine components (with the same dynamics as described previously) as follows:

1) baseline activity (constant),
2) HP limb position sensitivity for extension,
3) HP limb position sensitivity for flexion,
4) HP limb velocity sensitivity for extension,
5) HP limb velocity sensitivity for flexion,
6) rectified HP roll position sensitivity,
7) HP roll velocity sensitivity (unrectified, ipsilateral ear up positive),
8) rectified LP limb position sensitivity, and
9) rectified LP roll position sensitivity.

Graphical (visualization of the scatterplot matrix, Fig. 4) and linear regression analysis revealed the sensitivities of the high pass roll velocity (unrectified) and rectified high pass roll position processes are highly correlated (adjusted R^2 = 0.674), with the sensitivity of the former equal to 0.291 times the latter with no constant term.

A "third iteration" of model parameter estimation confirmed a strong linear relationship (adjusted R^2 = 0.605) between the baseline activity parameter and the rectified low pass limb position sensitivity (note that this relationship is evident the second iteration, Fig. 4 parameters 1 and 8), estimated by regression analysis as 23.441 − 5.163 × rectified low pass limb position sensitivity.

After a "fourth iteration" of parameter estimation, the scatterplot matrix and linear regression revealed a single significant relationship (adjusted R^2 = 0.36) for the high pass limb velocity extension and flexion sensitivities. The latter sensitivity was equal to 0.402 (±0.075) times the former.

The "final form" of the model for functional unit analysis was the weighted sum of the following nine component signals:

1) baseline activity (constant − 5.163 × rectified LP limb position sensitivity),
2) HP limb position sensitivity for extension,
3) HP limb position sensitivity for flexion,
4) HP limb velocity sensitivity for extension (residual),
5) HP limb velocity sensitivity for flexion − 0.402 × HP limb extension velocity sensitivity,
6) rectified HP roll position sensitivity + 0.291 × HP roll velocity sensitivity (ipsilateral ear up positive),
7) residual HP roll velocity sensitivity (unrectified, ipsilateral positive),
8) rectified LP limb position sensitivity − 5.68 sp/s (a constant to adjust its set point), and
9) rectified LP roll position sensitivity.

The final scatterplot matrix and regression analyses showed no significant correlations, indicating an uncorrelated basis set of components (Fig. 4).

Histologic Analysis

After the completion of data collection from each animal, two electrolytic lesions were made near the recording sites in the brainstem by passing a 0.5–1 mA current through a low impedance (0.5 MΩ) electrode for up to 60 s. Electrolytic lesions were allowed to mature for 7 days before euthanasia. Animals were deeply sedated with an initial intramuscular injection of ketamine (20 mg/kg) and acepromazine (0.2 mg/kg) followed by an intraperitoneal injection of pentobarbital sodium (40 mg/kg) and then perfused transcardially with 10% formalin. The brainstem was removed, fixed in 10% formalin, embedded in 2% agar, and cut transversely at a thickness of 50 μm using a freezing microtome. Sections were stained with 1% thionine. Recording locations were reconstructed with reference to the electrolytic lesions, the relative positions of the recording tracks, and the relative depths of the units.

RESULTS

Complete data were obtained from 129 VN units of four conscious cats. Composite response histograms were generated for each unit, and the response histograms were fit by an additive model of low- and high-pass filtered limb and body position signals using least squares nonlinear regression as outlined in the METHODS section (Fig. 5). This additive model for roll and limb stimulation described the discharges of the population of units with high fidelity. The mean R^2 value for goodness of fit across all units was 0.74 ± 0.17 (range, 0.31–0.98). The distribution of the R^2 values is shown in Fig. 6 and was negatively skewed (skew statistic, −0.484).

Vestibular Dynamics

The vestibular dynamics are represented robustly by a signal comprised of a linear combination of the rectified high pass roll position and velocity subcomponents; the sensitivity to this variable will hereafter be referred to as "vestibular sensitivity." It will be expressed as a scaling factor in

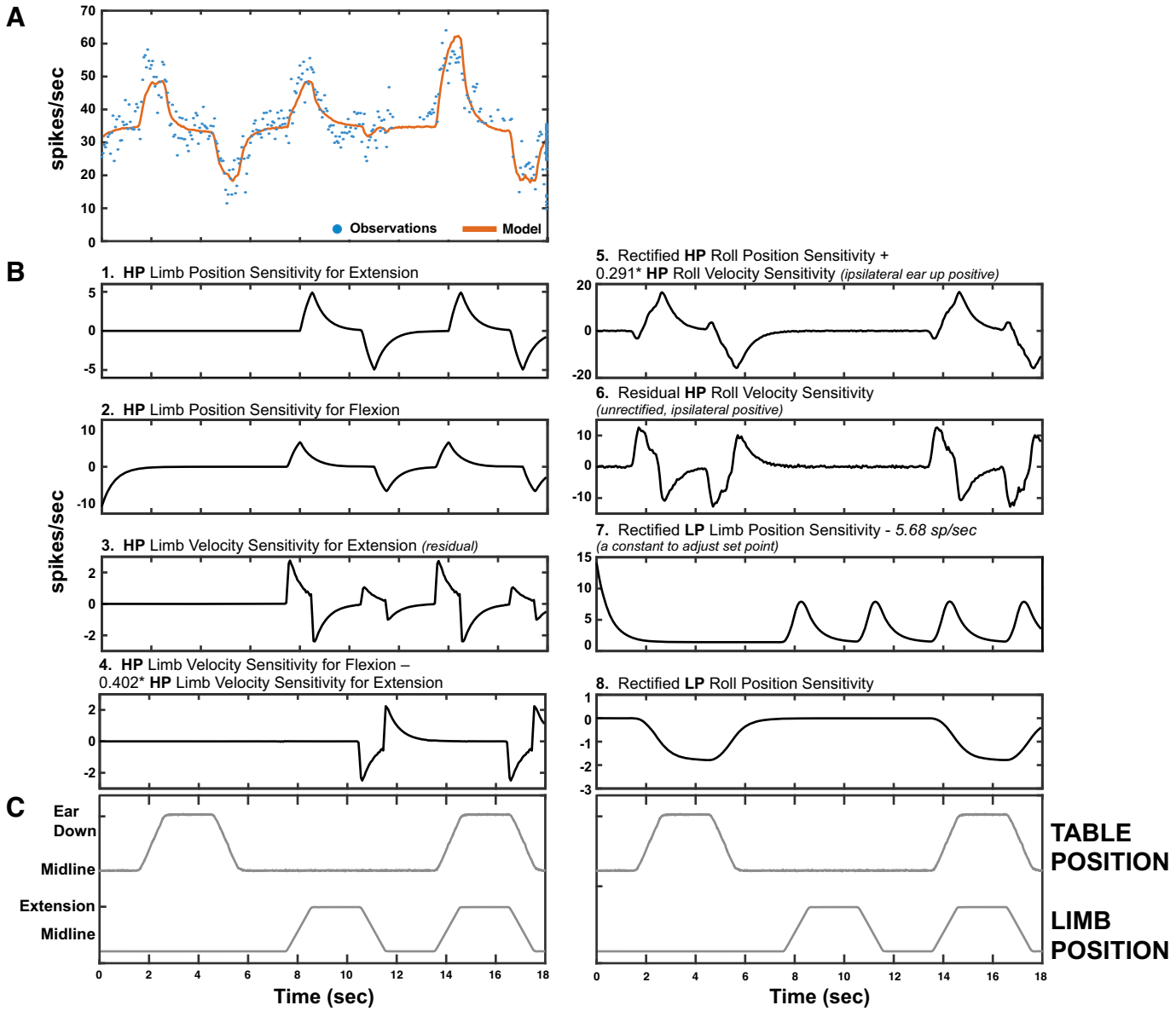

Figure 5. An example response of a vestibular nucleus (VN) neuron to roll body rotation, hindlimb movement, and both movements delivered simultaneously. The response to simultaneous delivery of roll and limb stimuli results from the weighted sum of the individual components. *A*: the observed firing rate (blue dots) and the modeled firing rate (orange solid line, see *Iterative Modeling Strategy for Vestibular and Limb Signal Identification*) are shown. *B*: the individual signal components for the unit in *A* are plotted (with the exception of baseline firing rate, which is a flat line). *C*: limb and table position. HP, high pass; LP, low pass.

spikes/s, relative to the output of the model of the component to the position and velocity of the input profile. The signal was identified through a stepwise elimination of the partial correlations of covarying components, and thus carries a substantial amount of the vestibular sensitivity. All cells in our data set had nonzero estimates for this parameter. Note that parameters representing other vestibular dynamics were also in the final model; those parameters followed similar distributions as shown for this variable.

We investigated the magnitude of the vestibular responses, irrespective of polarity or directionality, by taking the absolute value of the sensitivity of this component. The distribution of the absolute sensitivity reveals an exponential distribution with a rate parameter (λ) of 0.390. We divided the distribution into three distinct sensitivity classes based on the reciprocal of the rate parameter (Table 1):

$$\text{Low absolute vestibular sensitivity} \leq \frac{1}{\lambda};$$

$$\frac{1}{\lambda} < \text{intermediate vestibular sensitivity} \leq \frac{2}{\lambda};$$

$$\text{high absolute vestibular sensitivity} > \frac{2}{\lambda}.$$

The majority of neurons (63.6%) were classified into the low absolute vestibular sensitivity category (82/129 neurons). The mean sensitivity for these neurons was 0.969 ± 0.741 spikes/s, and sensitivities ranged from a minimum of 0.006

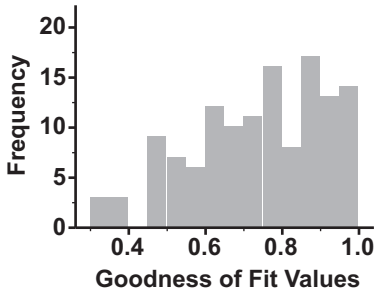

Figure 6. A histogram of the distribution of R^2 values for the fit of an additive model of low and high pass filtered limb and table movement dynamics (indicative of limb proprioceptive and vestibular signals, respectively) using least squares nonlinear regression to neural firing of individual vestibular nucleus (VN) neurons.

to a maximum of 2.538 spikes/s. Approximately 21% of neurons were classified as having intermediate absolute vestibular sensitivity (20.9%; 27/129 neurons). These neurons had vestibular sensitivities ranging from 2.625 to 5.067 spikes/s (means ± SD, 3.507 ± 0.628 spikes/s). The remaining 15.5% of neurons were classified as having high absolute vestibular sensitivity (20/129 neurons). Vestibular sensitivity values for neurons in this category ranged from 5.284 to 13.755 spikes/s, and the mean was 7.814 ± 2.236 spikes/s.

LP Limb Position Dynamics

Dynamics of the response to low pass limb movement are represented well by a LP limb position sensitivity signal (rectified low pass limb position − 5.68 spikes/s). The sensitivity to this variable will hereafter be referred to as "LP limb position sensitivity." It will be expressed as a scaling factor in spikes/s, relative to the output of the model to the position of the input profile (in this case, spikes/s/deg). The absolute value of the sensitivities of neuronal responses to this signal revealed an exponential distribution with a rate parameter (λ) of 0.314. The distribution was divided into three distinct classes based on the reciprocal of the rate parameter (Table 1):

$$\text{Low absolute LP limb position sensitivity} \leq \frac{1}{\lambda};$$

$$\frac{1}{\lambda} < \text{intermediate LP limb position sensitivity} \leq \frac{2}{\lambda};$$

$$\text{high absolute LP limb position sensitivity} > \frac{2}{\lambda}.$$

About two-thirds of the neurons were classified into the low absolute sensitivity to limb movement category (66.7%, 86/129 neurons). Neurons with intermediate absolute limb sensitivity were the next most common group, representing approximately 21% (20.9%; 27/129 neurons) of all neurons. Finally, neurons in the high absolute sensitivity classification were least common (12.4%, 16/129 neurons). Neuronal absolute LP limb position sensitivities are shown categorized by group in Table 1.

Combined Vestibular and LP Limb Position Sensitivities

Neurons could be further divided into nine groups on the basis of vestibular and low pass limb position sensitivities (Fig. 7*A*; Table 2). The most common unit responses (54/129 units; 41.9%) were neurons with low absolute vestibular and LP limb position sensitivities (Fig. 7*B*, *1*). Intermediate absolute vestibular–low absolute limb sensitivity neurons (17/129 units; 13.2%; Fig. 7*B*, *4*) and low absolute vestibular–intermediate absolute limb sensitivity neurons (14/129, 10.9%; Fig. 7*B*, *2*) were the next most common subcategories. High absolute vestibular–low absolute limb sensitivity neurons were robustly sensitive to vestibular stimulation but were minimally responsive to limb movement; they made up 11.6% (15/129 neurons; Fig. 7*B*, *7*) of the population. On the opposite end of the spectrum, low absolute vestibular–high absolute limb sensitivity neurons (14/129 neurons; 10.9%; Fig. 7*B*, *3*) were preferentially responsive to limb movement. The remaining four groups represented 11.6% of the neurons. Intermediate absolute vestibular–intermediate absolute limb sensitivity neurons made up seven percent of the population (9/129 neurons; Fig. 7*B*, *5*). A single neuron had intermediate absolute vestibular–high absolute limb sensitivity (0.8%; Fig. 7*B*, *6*). Four neurons (3.1%) were highly sensitivity to vestibular stimulation and had intermediate sensitivity to limb movement (Fig. 7*B*, *8*). Finally, one neuron was classified as having high absolute vestibular–high absolute limb sensitivity (0.8%; Fig. 7*B*, *9*). In summary, although the majority of neurons had low sensitivity to both parameters, a subset of neurons showed high sensitivity toward either vestibular or LP limb sensitivity.

HP Limb Velocity Dynamics

Dynamics of the response to high pass limb movement are represented well by the HP limb velocity sensitivity signal (HP limb velocity sensitivity for flexion − 0.402 × HP limb extension velocity sensitivity). The sensitivity to this variable will hereafter be referred to as "HP limb velocity sensitivity." It will be expressed as a scaling factor in spikes/s, relative to the output of the model to the velocity of the input profile (in this case, spikes/s per deg/s).

Table 1. *Vestibular and limb sensitivities of vestibular nucleus neurons*

	Subclass	Count	Mean	SD	Min	Max
Absolute vestibular sensitivity, spikes/s	Low	82	0.969	0.741	0.006	2.538
	Intermediate	27	3.507	0.628	2.625	5.067
	High	20	7.814	2.236	5.284	13.755
Absolute low pass limb position sensitivity, spikes/s	Low	86	1.256	0.853	0.002	3.170
	Intermediate	27	4.541	0.993	3.279	6.340
	High	16	11.259	6.315	6.571	25.954
Absolute high pass limb velocity sensitivity, spikes/s	Low	90	0.092	0.064	0.002	0.227
	Intermediate	20	0.327	0.067	0.245	0.438
	High	19	0.764	0.238	0.475	1.371

Categorization of responses to this signal showed a similar distribution to that of the vestibular and LP limb position sensitivity signals. The absolute value of the HP limb velocity sensitivity followed an exponential distribution with a rate parameter (λ) of 4.401. As with vestibular sensitivity and LP limb sensitivity, the HP limb velocity distribution was divided into three sensitivity classes based on the reciprocal of the rate parameter (Table 1).

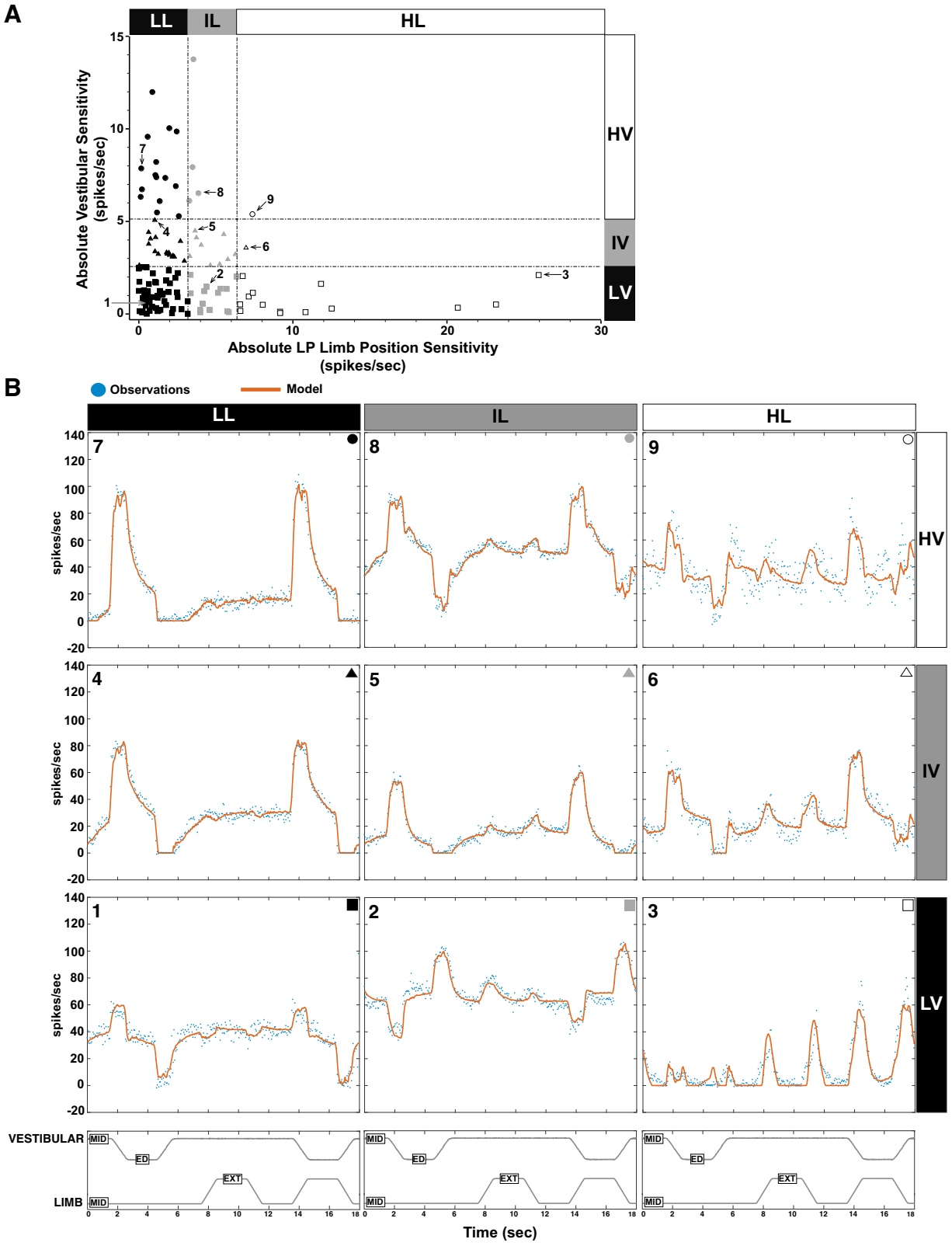

Table 2. *Vestibular and limb sensitivities of vestibular nucleus neurons by subclassification*

			Absolute Vestibular Sensitivity, spikes/s				Absolute LP Limb Position Sensitivity, spikes/s			
Class	%	Count	Mean	SD	Min	Max	Mean	SD	Min	Max
LL	41.9%	54	1.034	0.756	0.006	2.538	1.158	0.865	0.002	3.170
LI	10.9%	14	0.938	0.711	0.088	2.115	4.729	0.953	3.355	6.340
LH	10.9%	14	0.750	0.717	0.053	2.106	11.844	6.562	6.571	25.954
IL	13.2%	17	3.522	0.624	2.625	5.067	1.557	0.814	0.033	2.956
II	7.0%	9	3.472	0.708	2.627	4.490	4.692	1.059	3.307	6.270
IH	0.8%	1	3.574		3.574	3.574	6.958		6.958	6.958
HL	11.6%	15	7.771	1.875	5.284	11.987	1.266	0.827	0.122	2.598
HI	3.1%	4	8.579	3.537	6.110	13.755	3.546	0.243	3.279	3.867
HH	0.8%	1	5.392		5.392	5.392	7.372		7.372	7.372

HH, high vestibular-high limb; HI, high vestibular- intermediate limb; HL, high vestibular-low limb; IH, intermediate vestibular-high limb; II, intermediate vestibular-intermediate limb; IL, intermediate vestibular-low limb; LH, low vestibular-high limb; LI, low vestibular-intermediate limb; LL, low vestibular-low limb.

Combined LP Limb Position and HP Limb Velocity Sensitivities

One gains a more comprehensive view of the encoding of limb and vestibular information by considering the relationships among LP limb position and HP limb velocity sensitivities across units with different vestibular sensitivities. Fuzzy cluster analysis (44) (using "fcm.m" in MATLAB) of the relationship between low pass limb position and high pass limb velocity sensitivities identified three groups of units in log-log plots (Fig. 8), which we term high (asterisks), intermediate (plus signs), and low (triangles) combined limb sensitivity. Each of these groups contained units with low (black), intermediate (green), and high (red) vestibular sensitivity. Examples of the responses of these units are shown in Fig. 9. Note that across the range of limb sensitivity of the units, the discharges during hindlimb stimulation are well within their respective dynamic modulation ranges.

The intermediate and high hindlimb sensitivity units showed a fractional exponential relationship for low pass position and high pass velocity signal content, indicated by the regression line in Fig. 8. The domain spanned almost two orders of magnitude for high pass limb velocity sensitivity, whereas the range spanned a little over one order of magnitude for low pass limb position sensitivity. This relationship indicates that the responses of the units with high limb sensitivity (Fig. 8, asterisks) have a sharper onset to hindlimb extension and flexion (relatively more high pass signals; Fig. 9, upper row) than do the units with intermediate hindlimb sensitivity (Fig. 8, plus signs; Fig. 9, second row). The prominent high pass velocity signal of the more sensitive units will detect changes in length rapidly; the low pass position signal will give a slower signal reflecting final length (or position) in the units. Specifically, for a low magnitude hindlimb proprioceptive input, only the most sensitive units will respond with a profile that has a pronounced high pass velocity component (Fig. 9, upper row of units) that produces a rapid rise in firing rate. For higher magnitude hindlimb proprioceptive inputs, the high pass velocity component is less pronounced and the initial rise in the response rate is less sharp (Fig. 9, rows 2 and 3). When the data are rotated so that this line is the abscissa, the units are distributed uniformly along the relationship range (Kolmogorov–Smirnov test versus uniform distribution, $P > 0.5$) and the symmetric dispersion along the ordinate is consistent with a Gaussian distribution (Lilliefors Kolmogorov–Smirnov test, $P = 0.49$). These distributional features imply that the number of recruited units during a limb movement will scale directly with the logarithm of the magnitude and dynamics (velocity) of the movement.

Baseline Firing Rate

The estimated baseline firing rates of vestibular nucleus neurons ranged from −34 to 116 spikes/s and followed a normal distribution (means ± SD, 24 ± 20 spikes/s). Approximately 7% (9/129) of neurons had a zero or negative estimated baseline firing rate. Neurons with a zero or negative baseline firing rate were silent and responded only during vestibular or limb stimulation, suggesting that they were under tonic inhibition (e.g., Fig. 7*B*, *3*). The remaining 120 units had a positive estimated baseline firing rate. Like vestibular afferents, a positive baseline firing rate permits the neurons to display directional tuning. The baseline firing rate did not appear to differ as a function of either the magnitude of the absolute vestibular sensitivity (Fig. 10*A*), the magnitude of the absolute LP limb position sensitivity (Fig. 10*B*), or the magnitude of the absolute HP limb velocity sensitivity (Fig. 10*C*).

Location of VN Units

The physiological data were obtained from 129 units recorded from the brainstem of four conscious felines. The locations of recorded neurons were plotted with respect to an electrolytic lesion made in the same tract or in an adjacent track. It was possible to accurately reconstruct the

Figure 7. *A*: neurons could be further divided into nine groups on the basis of vestibular and low pass limb position sensitivities. Units labeled 1 through 9 correspond to the example units shown in *B*. *B*: the averaged responses of nine units represent the salient features of vestibular nucleus (VN) neuron responses to combined vestibular and hindlimb stimulation. The observed firing rate (blue dots) and the modeled firing rate (the fit of the model to the data; orange solid line, see *Iterative Modeling Strategy for Vestibular and Limb Signal Identification*) are shown for each unit. 7–9: units classified as having high absolute vestibular sensitivity; 4–6: units have intermediate absolute vestibular sensitivity; 1–3: units have low absolute vestibular sensitivity. Units 1, 4, and 7 have low absolute LP limb position sensitivity, units 2, 5, and 8 have intermediate absolute LP limb position sensitivity, whereas units 3, 6, and 9 have high absolute LP limb position sensitivity. ED, ear down; EXT, extension; HL, high limb; HV, high vestibular; IL, intermediate limb; IV, intermediate vestibular; LL, low limb; LP, low pass; LV, low vestibular; MID, midline.

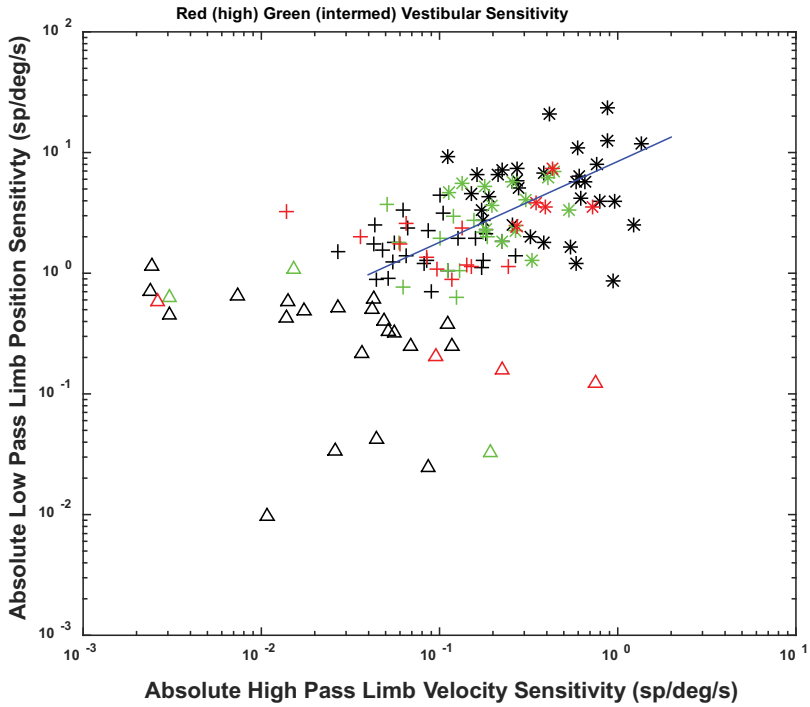

Figure 8. Plot of low pass (LP) limb position sensitivity vs. high pass (HP) limb velocity sensitivity on a log-log scale. Fuzzy cluster analysis reveals three groups of units, which we term high (*), intermediate (+) and low (△) combined limb sensitivity. Vestibular sensitivity of units is shown superimposed on these units by color with high sensitivity being shown as red, intermediate as green, and low as black. A fractional exponential relationship for LP limb position and HP limb velocity sensitivities was detected (shown as regression line on chart).

location of 88 neurons. These 88 neurons were histologically confirmed to be located within the lateral, medial, and inferior vestibular nuclei (Fig. 11). Units were scattered over a rostrocaudal extent of 2.1–7.5 mm (mean 5.5 ± 1.8 mm) rostral to the obex and were on average, 2.6 ± 1.0 mm lateral to the midline (range: 0.5–5.3 mm). Lesions were not well formed in one animal (accounting for 41 neurons in the data set), we thus relied on scarring from recording tracks to plot out the locations of recorded units. In this animal, units were located over of a similar spread of territory [distance rostral to the obex: 3.3–8.1 mm (5.8 ± 1.1 mm); distance lateral to the midline: 1–4 mm (3.0 ± 0.8 mm)] as the other three animals. Because we were not able to definitively confirm locations within the specific vestibular subnuclei relative to lesion sites in this animal, these data are not plotted on Fig. 11.

DISCUSSION

Our findings demonstrate that vestibular nucleus neurons integrate information from hindlimb proprioceptive inputs with information from peripheral vestibular receptors. We found that VN neuronal activity during combined vestibular and hindlimb proprioceptive stimulation in the conscious cat is well fit by a simple additive model for signals with similar temporal dynamics. The average R^2 goodness-of-fit value for fitting the additive model to neural firing was 0.74, with very few model fits being in the lower range (Fig. 6). The ability to integrate multimodal sensory signals is a key feature of neurons in the central nervous system that participate in balance control and is particularly notable among those in the vestibular nuclei (1–4, 8, 12, 45). Convergence of proprioceptive signals with vestibular signals commonly occurs among vestibular nucleus neurons. For instance, in cats and squirrel monkeys a substantial majority (~80%) of vestibular nucleus neurons were found to have their activity modulated with activation of neck proprioceptive afferents and those neck proprioceptive signals integrated with vestibular inputs in an additive fashion (32, 33, 46–49). Our group has previously demonstrated that over two-thirds of vestibular nucleus neurons in conscious cats have their activity modulated by hindlimb movement (31). The present work extends those previous findings by demonstrating that limb proprioceptive signals integrate with vestibular signals in an additive fashion. As proprioceptive inputs from the neck and hindlimb each converge and integrate with vestibular inputs in the vestibular nuclei in an additive manner, it is likely that proprioceptive inputs from throughout the body are similarly processed in an additive manner by the vestibular nuclei (note, however, that this assumption has yet to be explicitly tested). This suggests that vestibular nucleus neurons may process vestibular afferent information in the context of position and movement of the whole body in space, rather than solely in a "head-referenced" frame (50, 51). This is likely especially true of vestibular nucleus neurons with spinal projections that influence motor outflow in response to perturbations.

Although our final model included eight vestibular and limb related signal components and one baseline component, we chose to focus our analysis on the dynamics from three main components: vestibular sensitivity [rectified HP roll position sensitivity + 0.291 × HP roll velocity sensitivity (ipsilateral ear up positive)], LP limb position sensitivity [rectified LP limb position sensitivity − 5.68 sp/s (a constant to adjust its set point)] and HP limb velocity sensitivity (HP limb flexion velocity sensitivity − 0.402 × HP limb extension velocity sensitivity) because these terms included features

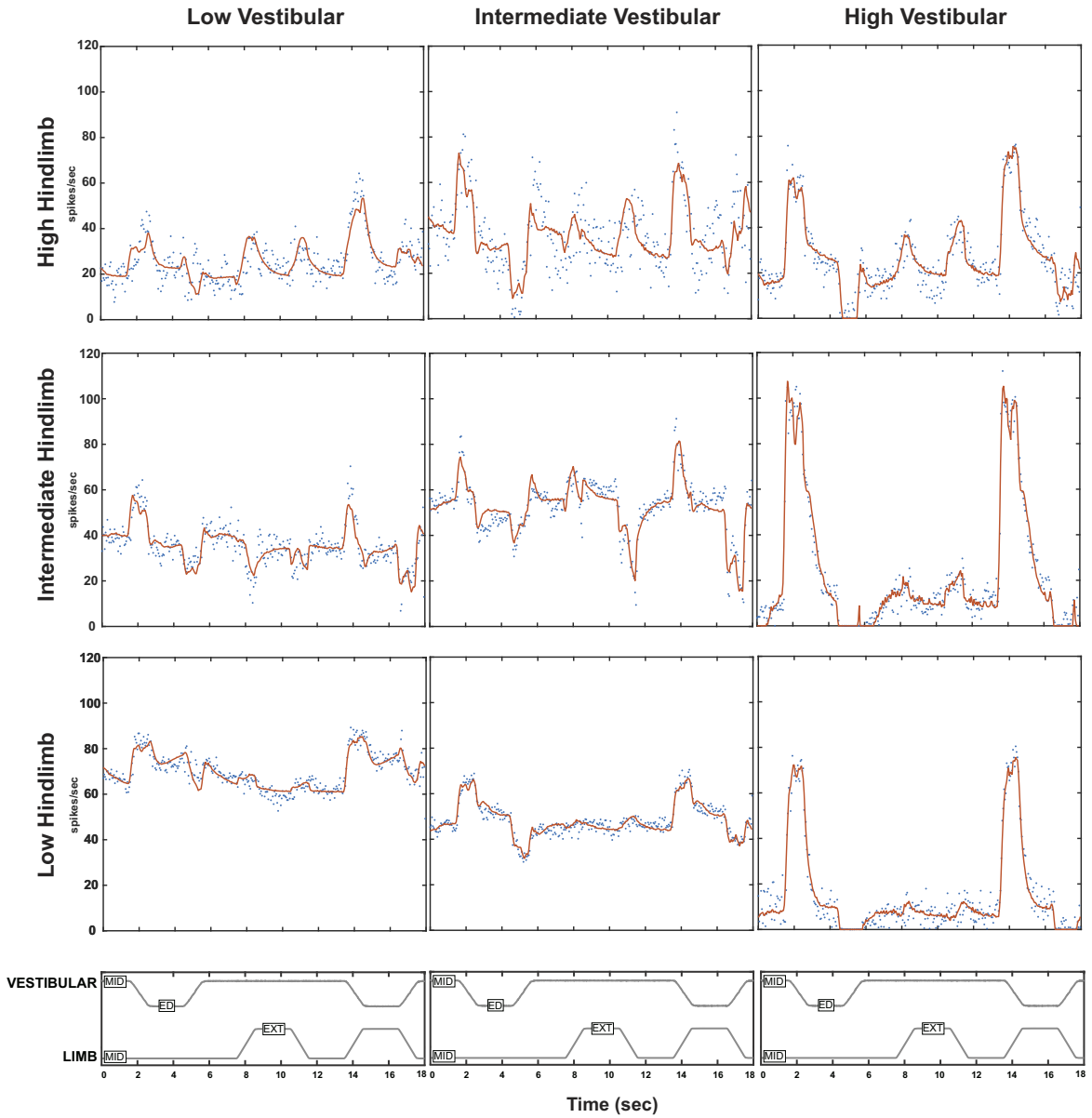

Figure 9. Examples of unit responses summarized in Fig. 8. The stimulus profile for whole body roll (MID designates static in horizonal plane, ED designates ear down tilt) and hindlimb movement (MID designates resting position, EXT indicates extension) shown in the *top* panels. The unit spike response rates are shown in blue and the red curves show the model fit (including parameters graphed in Fig. 8), The units are organized to show the vestibular and hindlimb proprioceptive response components and their additivity. The columns are arranged by increasing vestibular sensitivity (high indicated by red symbols in Fig. 8, intermediate by green symbols, low by black symbols). The rows indicate different levels of hindlimb sensitivity (in Fig. 8; high indicated by *, intermediate by +, and low by △). ED, ear down; EXT, extension; LP, low pass; MID, midline.

that were thought to be most representative of the underlying stimuli.

The vestibular sensitivity term selected for in-depth analysis is thought to represent a processed signal containing inputs originating from both semicircular canal and otolith afferents. Roll plane stimulation was chosen because it has previously been demonstrated that the vast majority of neurons receiving converging vestibular and hindlimb inputs have response vector orientations within 45° of the roll plane (30, 31). Semicircular canal and dynamic otolith afferents likely drive the high pass roll velocity signal. The semicircular canals have high-pass filtering properties, and due to the fluid mechanics of the canals, responses of canal afferents approach being in phase with the velocity of rotation across many stimulus frequencies (52). Although semicircular canals have dynamic components, otolith units have both dynamic and static components (53). Phasic-tonic otolith afferents have a dynamic component that scales with increasing ramp velocity and a static positional component during the hold period (53). The rectified high pass roll position signal is likely a highly processed otolith signal. Evidence from nonhuman primates shows that there is substantial spatiotemporal processing of otolith afferent signals by vestibular nucleus neurons (54). In the case of the limb

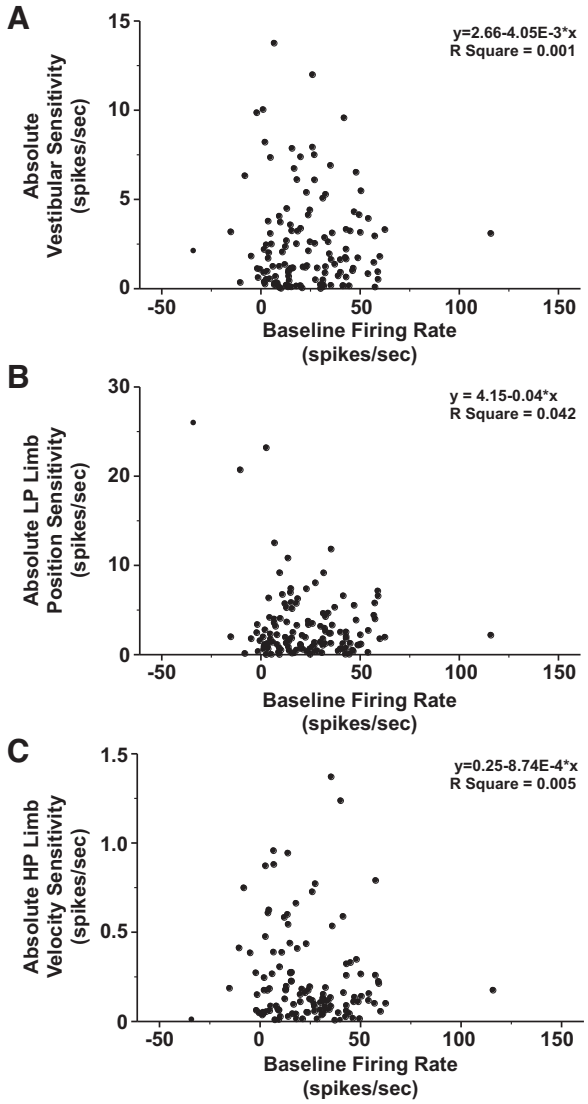

Figure 10. The baseline firing rate was not correlated with the absolute vestibular sensitivity (*A*), absolute low pass (LP) limb position sensitivity (*B*), or absolute HP limb velocity sensitivity (*C*). The regression equation and R^2 value for each subplot are indicated in the upper right of the subplot.

terms, selecting representative terms was moderately more challenging because, unlike vestibular inputs, little is presently known about which specific proprioceptive receptors (muscle spindles, cutaneous receptors, Golgi tendon organs, etc.) are responsible for signaling limb-state changes to the vestibular nuclei. However, responses of vestibular nucleus neurons in the conscious cat have a strong phasic component during limb movement and, in some cases, a lasting positional component (31), which are well approximated by the HP limb velocity term and LP limb position term, respectively.

Sensitivities of vestibular nucleus neurons to individual components of the additive model took the form of exponential functions, excepting estimated baseline firing rate, with the majority of neurons exhibiting low sensitivity to a given component and relatively few being highly sensitive. Interestingly, neurons with high sensitivity to one domain were unlikely to also have high sensitivity in a cross-modal domain. For example, as shown in Fig. 7, most neurons that were in the high category of LP limb position sensitivity were in the low category of vestibular sensitivity and vice versa. These findings suggest that while a large majority of the population of vestibular nucleus neurons appear fairly broadly tuned to cross-modality stimuli, some subpopulations of neurons appear to be tuned to extract particular salient features of the stimuli in one modality. When viewed as a population of neurons that is attempted to discern input characteristics of a given stimulus, having neurons that excel at encoding particular features of the stimulus could allow for subcortical sensory processing of salient features leading to balance percepts. Note, however, that although seemingly useful, having distinct response properties to salient features of a stimulus is not a necessary feature for subcortical sensory perceptual processing. Jorntell et al. (45) recently demonstrated that salient features of skin-object interactions were encoded by neurons in the cuneate nucleus despite having similar underlying response properties and receptive fields.

Power law scaling has been reported widely for psychophysical measurements of sensations (55), including scaling of high pass and low pass pain sensation for topical capsaicin

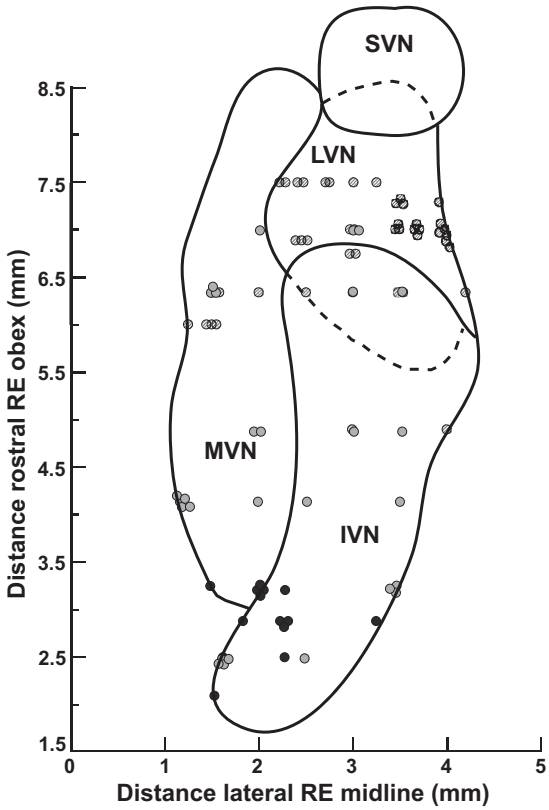

Figure 11. A horizontal section through the vestibular nucleus complex showing the location of neurons whose activity was recorded in this study. The *y*-axis designates the distance in millimeters rostral to the obex, and the distance in millimeters lateral to the midline is shown on the *x*-axis. The activity of neurons was recorded over a rostral-caudal distance of 6 mm, from 2.1 mm to 8.1 mm rostral to the obex. Symbol shading indicates neurons recorded from different cats. IVN, inferior vestibular nucleus; LVN, lateral vestibular nucleus; MVN, medial vestibular nucleus; RE, relative to; SVN superior vestibular nucleus.

(56). A power law scaling was observed in these data for low pass limb position and high pass limb velocity sensitivity across units (Fig. 8), which was independent of their vestibular sensitivities. The sampled units were also distributed uniformly along this relationship, suggesting that the number of active units and their response dynamics will vary systematically with the movement trajectory. For example, an order of recruitment effect is clear in results of limb responses from the right column of Fig. 9. The high combined limb sensitivity units (enhanced high pass limb velocity sensitivity) respond with the shortest latency during the extension and flexion periods, with longer latencies and smaller responses for the intermediate and low limb sensitivity units. From an information perspective, the high sensitivity responses are indicating the rate of change in limb length whereas the less sensitive units give information about the magnitude of the change in length; the ensemble of the unit activities give a more comprehensive picture of the limb trajectory over the time scale of the movement. On the other hand, short duration, small perturbations of limb position will produce transient activation of the most sensitive units, reflecting primarily the rate of dynamic change in flexion or extension.

It is important to remember that the data generated in this study were all from passively applied limb movements, and thus the responses elicited in the vestibular nuclei were in response to exafferent signals. Because of this fact, one reasonable hypothesis to consider is that the information encoded by VN neurons in response to passive limb movement serves to prime vestibulospinal reflexes during destabilizing postural occurrences, in particular those that result in coactivation of vestibular and limb afferents. An example of such a situation where this may be beneficial is a person walking on a sidewalk and unexpectedly encountering black ice. In such a situation, when the lower limb slips, a limb exafferent signal would be generated concurrent with an exafferent signal from vestibular afferents due to the co-occurring resultant head movement in space. Such a situation would call for rapid postural adjustments in an attempt to maintain upright stance, and as such, a primed vestibulospinal response would be warranted. Active (self-generated) hindlimb muscle contraction can also modulate the activity of vestibular nucleus neurons (31); however it remains unclear if the resultant modulation under those conditions is from reafference or efference copy. As the present study did not examine for integration of limb proprioceptive signals with vestibular signals under conditions of active movement, it is presently unknown how these signals would influence vestibular nucleus neuronal activity during combined volitional limb and head movement, such as happens during locomotion (35). It is possible that integration of these signals would vary substantially during conditions of active movement, as has been seen in other studies examining the influence of signals from semicircular canals and otoliths on vestibular nucleus neuronal activity. During conditions of combined translation and rotation in nonhuman primates, the combined integrated signal is less during self-generated active movement than when these stimuli are passively applied (57). Future studies will be needed to determine how strongly signals are integrated in the vestibular nucleus during combined active limb and head movements.

One limitation of the current study is that felines are quadrupeds and it is likely that inputs from all four limbs are relayed to vestibular nucleus neurons, whereas our setup focused on inputs from only one limb. Vestibulospinal neuronal activity has previously been shown to modulate with the step-cycle in conscious cats in which all four limbs are in motion (58, 59). This finding raises the intriguing possibility that inputs from certain parts of the limbs, such as afferents innervating flexor or extensor muscle spindles, joint receptors, or cutaneous receptors may predominate at times depending upon movement about specific joints or activation of specific muscle groups with the step cycle. However, those experiments were carried out in head-free animals and thus the relative contribution of vestibular inputs was not able to be controlled for. Additional experiments are needed to explore how inputs from all four limbs integrate in the vestibular nuclei, particularly in head-fixed animals, under active and passive conditions. Another limitation of our experimental setup is that we did not define the projections of the vestibular nucleus neurons that we were recording from. It is likely that a large proportion of these neurons are vestibulospinal neurons that descend via the spinal cord to indirectly and directly influence motoneuron activity. Evidence from human studies shows that vestibulospinal reflexes are altered to account for lower limb (60, 61) and head position (1, 4, 9, 62–64). Moreover, exafferent vestibular stimulation modulates hindlimb EMG activity during locomotion and does so to each limb independently (65, 66). The neuronal responses we observed suggest vestibular nucleus neurons play a key role in mediating these responses. It is also possible that output information from vestibular nucleus neurons that integrate vestibular and limb proprioceptive information could influence other systems such as mediation of vestibuloautonomic reflexes (67), motor planning and execution through cerebellar projections, or project to cortical regions via vestibulothalamic pathways (68). Another important limitation with our experimental setup is that we used a restricted set of test parameters to facilitate the compliance of experimental animals. It remains to be determined if other stimulus conditions, such as vestibular and limb movements in different directions or velocities than tested here, would be well fit by an additive model. Moreover, the influences of other factors that can affect multisensory integration, such as attention (18–20), were not tested here.

In conclusion, neurons in the feline VN integrate inputs from the limb and labyrinth in an additive manner. We speculate that integration of these vestibular and limb signals by VN neurons serve to adjust vestibulospinal reflexes to account for limb position in space when a balance perturbation occurs. Further research will be needed to determine if this population of neurons has descending efferent projections down the spinal cord. This knowledge of how single neurons integrate sensory information across modalities is crucial to understanding how the vestibular system uses multimodal information to maintain balance in a dynamic environment.

ACKNOWLEDGMENTS

A preliminary report of these findings has been published on the *bioRxiv* preprint server (69).

GRANTS

This work was supported by National Institutes of Health (NIH) Grant K08-DC013571 (to A. A. McCall).

DISCLOSURES

No conflicts of interest, financial or otherwise, are declared by the authors.

AUTHOR CONTRIBUTIONS

A.A.M. and D.M.M. conceived and designed research; A.A.M. and D.M.M. performed experiments; A.A.M., D.M.M., and C.D.B. analyzed data; A.A.M., D.M.M., and C.D.B. interpreted results of experiments; D.M.M. prepared figures; A.A.M. and D.M.M. drafted manuscript; A.A.M., D.M.M., and C.D.B. edited and revised manuscript; A.A.M., D.M.M., and C.D.B. approved final version of manuscript.

REFERENCES

1. **Fitzpatrick R**, **Burke D**, **Gandevia SC.** Task-dependent reflex responses and movement illusions evoked by galvanic vestibular stimulation in standing humans. *J Physiol* 478: 363–372, 1994. doi:10.1113/jphysiol.1994.sp020257.
2. **Hlavacka F**, **Njiokiktjien C.** Postural responses evoked by sinusoidal galvanic stimulation of the labyrinth. Influence of head position. *Acta Otolaryngol* 99: 107–112, 1985. doi:10.3109/00016488509119152.
3. **Horak FB**, **Nashner LM**, **Diener HC.** Postural strategies associated with somatosensory and vestibular loss. *Exp Brain Res* 82: 167–177, 1990. doi:10.1007/BF00230848.
4. **Nashner LM**, **Wolfson P.** Influence of head position and proprioceptive cues on short latency postural reflexes evoked by galvanic stimulation of the human labyrinth. *Brain Res* 67: 255–268, 1974. doi:10.1016/0006-8993(74)90276-5.
5. **Berthoz A**, **Lacour M**, **Soechting JF**, **Vidal PP.** The role of vision in the control of posture during linear motion. *Prog Brain Res* 50: 197–209, 1979. doi:10.1016/S0079-6123(08)60820-1.
6. **Bronstein AM.** Suppression of visually evoked postural responses. *Exp Brain Res* 63: 655–658, 1986. doi:10.1007/BF00237488.
7. **Lee D**, **Lishman JR.** Visual proprioceptive control of stance. *J Hum Mov Stud* 1: 87–95, 1975.
8. **Waespe W**, **Henn V.** Neuronal activity in the vestibular nuclei of the alert monkey during vestibular and optokinetic stimulation. *Exp Brain Res* 27: 523–538, 1977. doi:10.1007/BF00239041.
9. **Allum JH.** Organization of stabilizing reflex responses in tibialis anterior muscles following ankle flexion perturbations of standing man. *Brain Res* 264: 297–301, 1983. doi:10.1016/0006-8993(83)90828-4.
10. **Anastasopoulos D**, **Bronstein A**, **Haslwanter T**, **Fetter M**, **Dichgans J.** The role of somatosensory input for the perception of verticality. *Ann N Y Acad Sci* 871: 379–383, 1999. doi:10.1111/j.1749-6632.1999.tb09199.x.
11. **Kavounoudias A**, **Gilhodes JC**, **Roll R**, **Roll JP.** From balance regulation to body orientation: two goals for muscle proprioceptive information processing? *Exp Brain Res* 124: 80–88, 1999. doi:10.1007/s002210050602.
12. **Meyer PF**, **Oddsson LI**, **De Luca CJ.** The role of plantar cutaneous sensation in unperturbed stance. *Exp Brain Res* 156: 505–512, 2004. doi:10.1007/s00221-003-1804-y.
13. **Angelaki DE**, **Cullen KE.** Vestibular system: the many facets of a multimodal sense. *Annu Rev Neurosci* 31: 125–150, 2008. doi:10.1146/annurev.neuro.31.060407.125555.
14. **Peterka RJ.** Sensorimotor integration in human postural control. *J Neurophysiol* 88: 1097–1118, 2002. doi:10.1152/jn.2002.88.3.1097.
15. **Jeka J**, **Oie KS**, **Kiemel T.** Multisensory information for human postural control: integrating touch and vision. *Exp Brain Res* 134: 107–125, 2000. doi:10.1007/s002210000412.
16. **Jeka J**, **Oie K**, **Schoner G**, **Dijkstra T**, **Henson E.** Position and velocity coupling of postural sway to somatosensory drive. *J Neurophysiol* 79: 1661–1674, 1998. doi:10.1152/jn.1998.79.4.1661.
17. **Maurer C**, **Mergner T**, **Peterka RJ.** Multisensory control of human upright stance. *Exp Brain Res* 171: 231–250, 2006. doi:10.1007/s00221-005-0256-y.
18. **Talsma D**, **Senkowski D**, **Soto-Faraco S**, **Woldorff MG.** The multifaceted interplay between attention and multisensory integration. *Trends Cogn Sci* 14: 400–410, 2010. doi:10.1016/j.tics.2010.06.008.
19. **Tang X**, **Wu J**, **Shen Y.** The interactions of multisensory integration with endogenous and exogenous attention. *Neurosci Biobehav Rev* 61: 208–224, 2016. doi:10.1016/j.neubiorev.2015.11.002.
20. **Zaback M**, **Carpenter MG**, **Adkin AL.** Threat-induced changes in attention during tests of static and anticipatory postural control. *Gait Posture* 45: 19–24, 2016. doi:10.1016/j.gaitpost.2015.12.033.
21. **Stevenson RA**, **Ghose D**, **Fister JK**, **Sarko DK**, **Altieri NA**, **Nidiffer AR**, **Kurela LR**, **Siemann JK**, **James TW**, **Wallace MT.** Identifying and quantifying multisensory integration: a tutorial review. *Brain Topogr* 27: 707–730, 2014. doi:10.1007/s10548-014-0365-7.
22. **Stein BE**, **Stanford TR.** Multisensory integration: current issues from the perspective of the single neuron. *Nat Rev Neurosci* 9: 255–266, 2008 [Erratum in *Nat Rev Neurosci* 9: 406, 2008]. doi:10.1038/nrn2331.
23. **Moayedi M**, **Davis KD.** Theories of pain: from specificity to gate control. *J Neurophysiol* 109: 5–12, 2013. doi:10.1152/jn.00457.2012.
24. **Seki K**, **Fetz EE.** Gating of sensory input at spinal and cortical levels during preparation and execution of voluntary movement. *J Neurosci* 32: 890–902, 2012. doi:10.1523/JNEUROSCI.4958-11.2012.
25. **Wiesman AI**, **Heinrichs-Graham E**, **Coolidge NM**, **Gehringer JE**, **Kurz MJ**, **Wilson TW.** Oscillatory dynamics and functional connectivity during gating of primary somatosensory responses. *J Physiol* 595: 1365–1375, 2017. doi:10.1113/JP273192.
26. **Meredith MA**, **Stein BE.** Visual, auditory, and somatosensory convergence on cells in superior colliculus results in multisensory integration. *J Neurophysiol* 56: 640–662, 1986. doi:10.1152/jn.1986.56.3.640.
27. **Perrault TJ, Jr.**, **Vaughan JW**, **Stein BE**, **Wallace MT.** Superior colliculus neurons use distinct operational modes in the integration of multisensory stimuli. *J Neurophysiol* 93: 2575–2586, 2005. doi:10.1152/jn.00926.2004.
28. **Stanford TR**, **Quessy S**, **Stein BE.** Evaluating the operations underlying multisensory integration in the cat superior colliculus. *J Neurosci* 25: 6499–6508, 2005. doi:10.1523/JNEUROSCI.5095-04.2005.
29. **Goldberg JM**, **Wilson VJ**, **Cullen KE**, **Angelaki DE**, **Broussard DM**, **Buttner-Ennever JA**, **Fukushima K**, **Minor LB.** *The Vestibular System: A Sixth Sense*. New York: Oxford University Press, 2012. doi:10.1093/acprof:oso/9780195167085.001.0001.
30. **Arshian MS**, **Hobson CE**, **Catanzaro MF**, **Miller DJ**, **Puterbaugh SR**, **Cotter LA**, **Yates BJ**, **McCall AA.** Vestibular nucleus neurons respond to hindlimb movement in the decerebrate cat. *J Neurophysiol* 111: 2423–2432, 2014. doi:10.1152/jn.00855.2013.
31. **McCall AA**, **Miller DM**, **DeMayo WM**, **Bourdages GH**, **Yates BJ.** Vestibular nucleus neurons respond to hindlimb movement in the conscious cat. *J Neurophysiol* 116: 1785–1794, 2016. doi:10.1152/jn.00414.2016.
32. **Wilson VJ**, **Yamagata Y**, **Yates BJ**, **Schor RH**, **Nonaka S.** Response of vestibular neurons to head rotations in vertical planes. III. Response of vestibulocollic neurons to vestibular and neck stimulation. *J Neurophysiol* 64: 1695–1703, 1990. doi:10.1152/jn.1990.64.6.1695.
33. **Gdowski GT**, **McCrea RA.** Neck proprioceptive inputs to primate vestibular nucleus neurons. *Exp Brain Res* 135: 511–526, 2000. doi:10.1007/s002210000542.
34. **Roy JE**, **Cullen KE.** Selective processing of vestibular reafference during self-generated head motion. *J Neurosci* 21: 2131–2142, 2001. doi:10.1523/JNEUROSCI.21-06-02131.2001.
35. **Zubair HN**, **Beloozerova IN**, **Sun H**, **Marlinski V.** Head movement during walking in the cat. *Neuroscience* 332: 101–120, 2016. doi:10.1016/j.neuroscience.2016.06.031.
36. **Miller DM**, **Cotter LA**, **Gandhi NJ**, **Schor RH**, **Cass SP**, **Huff NO**, **Raj SG**, **Shulman JA**, **Yates BJ.** Responses of caudal vestibular nucleus neurons of conscious cats to rotations in vertical planes, before and after a bilateral vestibular neurectomy. *Exp Brain Res* 188: 175–186, 2008. doi:10.1007/s00221-008-1359-z.

37. **Wilson VJ**, **Ikegami H**, **Schor RH**, **Thomson DB.** Tilt responses of neurons in the caudal descending nucleus of the decerebrate cat: influence of the caudal cerebellar vermis and of neck receptors. *J Neurophysiol* 75: 1242–1249, 1996. doi:10.1152/jn.1996.75.3.1242.
38. **Abelew TA**, **Miller MD**, **Cope TC**, **Nichols TR.** Local loss of proprioception results in disruption of interjoint coordination during locomotion in the cat. *J Neurophysiol* 84: 2709–2714, 2000. doi:10.1152/jn.2000.84.5.2709.
39. **Frigon A**, **Rossignol S.** Adaptive changes of the locomotor pattern and cutaneous reflexes during locomotion studied in the same cats before and after spinalization. *J Physiol* 586: 2927–2945, 2008. doi:10.1113/jphysiol.2008.152488.
40. **McCall AA**, **Miller DJ**, **Catanzaro MF**, **Cotter LA**, **Yates BJ.** Hindlimb movement modulates the activity of rostral fastigial nucleus neurons that process vestibular input. *Exp Brain Res* 233: 2411–2419, 2015. doi:10.1007/s00221-015-4311-z.
41. **Miller DM**, **DeMayo WM**, **Bourdages GH**, **Wittman SR**, **Yates BJ**, **McCall AA.** Neurons in the pontomedullary reticular formation receive converging inputs from the hindlimb and labyrinth. *Exp Brain Res* 235: 1195–1207, 2017. doi:10.1007/s00221-017-4875-x.
42. **Destefino VJ**, **Reighard DA**, **Sugiyama Y**, **Suzuki T**, **Cotter LA**, **Larson MG**, **Gandhi NJ**, **Barman SM**, **Yates BJ.** Responses of neurons in the rostral ventrolateral medulla to whole body rotations: comparisons in decerebrate and conscious cats. *J Appl Physiol (1985)* 110: 1699–1707, 2011. doi:10.1152/japplphysiol.00180.2011.
43. **Miller DM**, **Cotter LA**, **Gandhi NJ**, **Schor RH**, **Huff NO**, **Raj SG**, **Shulman JA**, **Yates BJ.** Responses of rostral fastigial nucleus neurons of conscious cats to rotations in vertical planes. *Neuroscience* 155: 317–325, 2008. doi:10.1016/j.neuroscience.2008.04.042.
44. **Bezdek JC.** *Pattern Recognition with Fuzzy Objective Function Algorithms*. New York: Plenum Press, 1981.
45. **Jorntell H**, **Bengtsson F**, **Geborek P**, **Spanne A**, **Terekhov AV**, **Hayward V.** Segregation of tactile input features in neurons of the cuneate nucleus. *Neuron* 83: 1444–1452, 2014. doi:10.1016/j.neuron.2014.07.038.
46. **Boyle R**, **Pompeiano O.** Convergence and interaction of neck and macular vestibular inputs on vestibulospinal neurons. *J Neurophysiol* 45: 852–868, 1981. doi:10.1152/jn.1981.45.5.852.
47. **Kasper J**, **Schor RH**, **Wilson VJ.** Response of vestibular neurons to head rotations in vertical planes. II. Response to neck stimulation and vestibular-neck interaction. *J Neurophysiol* 60: 1765–1778, 1988. doi:10.1152/jn.1988.60.5.1765.
48. **Kasper J**, **Thoden U.** Effects of natural neck afferent stimulation on vestibulo-spinal neurons in the decerebrate cat. *Exp Brain Res* 44: 401–408, 1981. doi:10.1007/BF00238832.
49. **McCrea RA**, **Gdowski GT**, **Boyle R**, **Belton T.** Firing behavior of vestibular neurons during active and passive head movements: vestibulo-spinal and other non-eye-movement related neurons. *J Neurophysiol* 82: 416–428, 1999. doi:10.1152/jn.1999.82.1.416.
50. **Brooks JX**, **Cullen KE.** Multimodal integration in rostral fastigial nucleus provides an estimate of body movement. *J Neurosci* 29: 10499–10511, 2009. doi:10.1523/JNEUROSCI.1937-09.2009.
51. **Green AM**, **Angelaki DE.** Internal models and neural computation in the vestibular system. *Exp Brain Res* 200: 197–222, 2010. doi:10.1007/s00221-009-2054-4.
52. **Fernandez C**, **Goldberg JM.** Physiology of peripheral neurons innervating semicircular canals of the squirrel monkey. II. Response to sinusoidal stimulation and dynamics of peripheral vestibular system. *J Neurophysiol* 34: 661–675, 1971. doi:10.1152/jn.1971.34.4.661.
53. **Anderson JH**, **Blanks RH**, **Precht W.** Response characteristics of semicircular canal and otolith systems in cat. I. Dynamic responses of primary vestibular fibers. *Exp Brain Res* 32: 491–507, 1978. doi:10.1007/BF00239549.
54. **Angelaki DE**, **Dickman JD.** Spatiotemporal processing of linear acceleration: primary afferent and central vestibular neuron responses. *J Neurophysiol* 84: 2113–2132, 2000. doi:10.1152/jn.2000.84.4.2113.
55. **McBurney DH**, **Balaban CD.** A heuristic model of sensory adaptation. *Atten Percept Psychophys* 71: 1941–1961, 2009. doi:10.3758/APP.71.8.1941.
56. **McBurney DH**, **Balaban CD**, **Popp JR**, **Rosenkranz JE.** Adaptation to capsaicin burn: effects of concentration and individual differences. *Physiol Behav* 72: 205–216, 2001. doi:10.1016/s0031-9384(00)00396-6.
57. **Carriot J**, **Jamali M**, **Brooks JX**, **Cullen KE.** Integration of canal and otolith inputs by central vestibular neurons is subadditive for both active and passive self-motion: implication for perception. *J Neurosci* 35: 3555–3565, 2015. doi:10.1523/JNEUROSCI.3540-14.2015.
58. **Matsuyama K**, **Drew T.** Vestibulospinal and reticulospinal neuronal activity during locomotion in the intact cat. I. Walking on a level surface. *J Neurophysiol* 84: 2237–2256, 2000. doi:10.1152/jn.2000.84.5.2237.
59. **Matsuyama K**, **Drew T.** Vestibulospinal and reticulospinal neuronal activity during locomotion in the intact cat. II. Walking on an inclined plane. *J Neurophysiol* 84: 2257–2276, 2000. doi:10.1152/jn.2000.84.5.2257.
60. **Grasso C**, **Barresi M**, **Scattina E**, **Orsini P**, **Vignali E**, **Bruschini L**, **Manzoni D.** Tuning of human vestibulospinal reflexes by leg rotation. *Hum Mov Sci* 30: 296–313, 2011. doi:10.1016/j.humov.2010.07.018.
61. **Welgampola MS**, **Colebatch JG.** Vestibulospinal reflexes: quantitative effects of sensory feedback and postural task. *Exp Brain Res* 139: 345–353, 2001. doi:10.1007/s002210100754.
62. **Ali AS**, **Rowen KA**, **Iles JF.** Vestibular actions on back and lower limb muscles during postural tasks in man. *J Physiol* 546: 615–624, 2003. doi:10.1113/jphysiol.2002.030031.
63. **Kennedy PM**, **Inglis JT.** Interaction effects of galvanic vestibular stimulation and head position on the soleus H reflex in humans. *Clin Neurophysiol* 113: 1709–1714, 2002. doi:10.1016/s1388-2457(02)00238-9.
64. **Kennedy PM**, **Inglis JT.** Modulation of the soleus H-reflex in prone human subjects using galvanic vestibular stimulation. *Clin Neurophysiol* 112: 2159–2163, 2001. doi:10.1016/S1388-2457(01)00665-4.
65. **Forbes PA**, **Vlutters M**, **Dakin CJ**, **van der Kooij H**, **Blouin JS**, **Schouten AC.** Rapid limb-specific modulation of vestibular contributions to ankle muscle activity during locomotion. *J Physiol* 595: 2175–2195, 2017. doi:10.1113/JP272614.
66. **Iles JF**, **Baderin R**, **Tanner R**, **Simon A.** Human standing and walking: comparison of the effects of stimulation of the vestibular system. *Exp Brain Res* 178: 151–166, 2007. doi:10.1007/s00221-006-0721-2.
67. **Yates BJ**, **Bolton PS**, **Macefield VG.** Vestibulo-sympathetic responses. *Compr Physiol* 4: 851–887, 2014. doi:10.1002/cphy.c130041.
68. **Lopez C**, **Blanke O.** The thalamocortical vestibular system in animals and humans. *Brain Res Rev* 67: 119–146, 2011. doi:10.1016/j.brainresrev.2010.12.002.
69. **Miller DM**, **Balaban CD**, **McCall AA.** Integration of vestibular and hindlimb inputs by vestibular nucleus neurons: multisensory influences on postural control (Preprint). *bioRxiv* 661736, 2019. doi:10.1101/661736.